Vol. 17, pp. 51–58 (2020)
doi: 10.2142/biophysico.BSJ-2020004

Biophysics and Physicobiology
https://www.jstage.jst.go.jp/browse/biophysico/

Review Article

Crystalline chitin hydrolase is a burnt-bridge Brownian motor

Akihiko Nakamura[1], Kei-ichi Okazaki[2], Tadaomi Furuta[3], Minoru Sakurai[3], Jun Ando[4] and Ryota Iino[2,5]

[1] *Shizuoka University, Shizuoka 422-8529, Japan*
[2] *Institute for Molecular Science, Okazaki, Aichi 444-8787, Japan*
[3] *Tokyo Institute of Technology, Yokohama, Kanagawa 226-8501, Japan*
[4] *RIKEN, Wako, Saitama 351-0198, Japan*
[5] *SOKENDAI, Hayama, Kanagawa 240-0193, Japan*

Received March 2, 2020; accepted May 27, 2020; Released online in J-STAGE as advance publication June 9, 2020

Motor proteins are essential units of life and are well-designed nanomachines working under thermal fluctuations. These proteins control moving direction by consuming chemical energy or by dissipating electrochemical potentials. Chitinase A from bacterium *Serratia marcescens* (SmChiA) processively moves along crystalline chitin by hydrolysis of a single polymer chain to soluble chitobiose. Recently, we directly observed the stepping motions of SmChiA labeled with a gold nanoparticle by dark-field scattering imaging to investigate the moving mechanism. Time constants analysis revealed that SmChiA moves back and forth along the chain freely, because forward and backward states have a similar free energy level. The similar probabilities of forward-step events (83.5%=69.3%+14.2%) from distributions of step sizes and chain-hydrolysis (86.3%=(1/2.9)/(1/2.9+1/18.3)×100) calculated from the ratios of time constants of hydrolysis and the backward step indicated that SmChiA moves forward as a result of shortening of the chain by a chitobiose unit, which stabilizes the backward state. Furthermore, X-ray crystal structures of sliding intermediate and molecular dynamics simulations showed that SmChiA slides forward and backward under thermal fluctuation without large conformational changes of the protein. Our results demonstrate that SmChiA is a burnt-bridge Brownian ratchet motor.

Key words: Brownian ratchet, molecular motor, single-molecule measurement, chitinase, biomass

Corresponding author: Akihiko Nakamura, Department of Applied Life Sciences, Faculty of Agriculture, Shizuoka University, 836 Ohya, Suruga-ku, Shizuoka 422-8529, Japan.
e-mail: aki-naka@shizuoka.ac.jp

Introduction

Complex functions of life are the results of chemical and physical reactions supported by enzymes [1]. Motor proteins such as kinesin [2], dynein [3], and myosin [4,5] transport a substance or generate a force by linear movement along with the rail proteins. In other cases, F_oF_1-ATP synthase generates ATP from a proton motive force [6] and V_oV_1-ATPase pumps ions [7,8] by rotating motions in a membrane. Investigations of the moving mechanisms of these enzymes are helpful to understand the biology or to design an artificial molecular motor.

Two major moving mechanisms were proposed previously [9]. One is "power stroke", in which enzymes move with a large conformational change of protein structures and rectify the direction of movement by changing the

◀ ***Significance*** ▶

Molecular motors need ATP or a chemical potential as the bias of moving direction. The major moving mechanisms are "power stroke" and "Brownian ratchet", and these two mechanisms are mixed in many cases. In this study, we revealed that a chitin hydrolase is a pure "burnt-bridge" Brownian ratchet motor, which creates a forward bias by shortening of the rail and inhibition of the backward movement. From the viewpoint of application, chitin is the second most abundant biomaterial on the Earth. Therefore, revealing the chitin degradation mechanism of chitinase is helpful to improve the utilization of chitin.

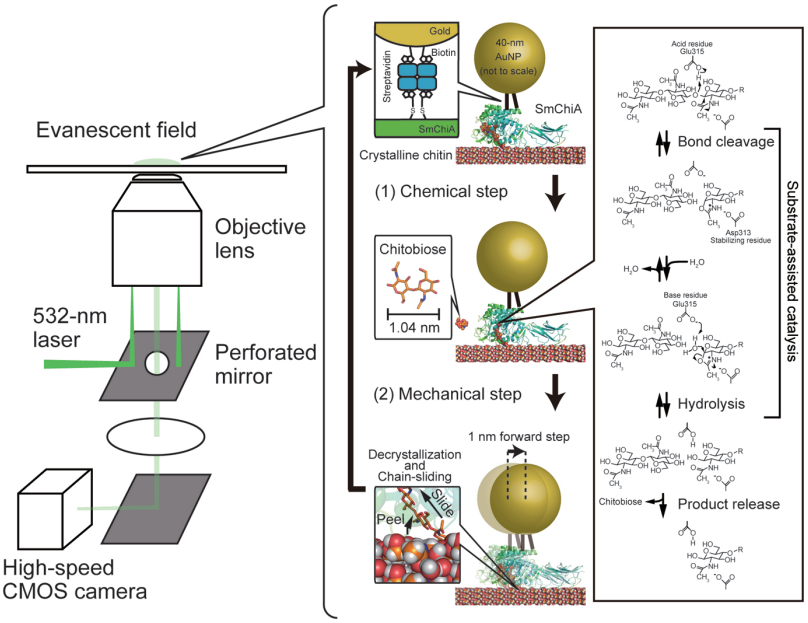

Figure 1 Setup of total internal reflection dark-field microscopy and the elementary catalytic steps of SmChiA labeled by a gold nanoparticle of 40-nm diameter.

position of equilibrium. The other mechanism is "Brownian ratchet", in which movement occurs under thermal fluctuation with rectified diffusion. To determine the mechanisms of molecular motors, single-molecule measurement is efficient. In particular, high-speed and high-precision measurement using plasmonic nano-probes is a promising method to investigate them. Gold nanoparticles with a diameter of several tens of nanometers are the most common probes, because they scatter green light very efficiently in water due to the localized surface plasmon resonance [10]. Free electrons in the gold nanoparticle are oscillated with the electromagnetic field of incident light. The oscillation of electrons induces an electric dipole, and the electrons move into the equilibrium position. This phenomenon causes absorption and scattering of the incident light. The electric field near the surface of the gold nanoparticle is greatly enhanced. A strong scattering signal from the gold nanoparticles is obtained without photobleaching. Therefore, Brownian motion of the kinesin head during the stepping motion can be observed [2].

Molecular motors working inside the cell or on a membrane usually use ATP as an energy source for their unidirectional movement. In contrast, hydrolases of cellulose and chitin (which are the main polysaccharides of the plant cell wall or exoskeleton of crustaceans and mycomycetes) move unidirectionally on the outside of the cell [11,12] and can even degrade stable crystalline substrates without utilizing ATP. In the research field of cellulase and chitinase, these degradation mechanisms with movements are called "processive reactions", which produce many disaccharides continuously per single binding event. Processive reactions are one of the main topics of research, because they are unique to enzymes that efficiently hydrolyze crystalline substrates. Their movements were first observed by high-speed atomic force microscopy (HS-AFM), and the movement, binding, and dissociation events were also verified by single-fluorescence microscopy. Notable examples include a cellulase from ascomycete *Trichoderma reesei* (TrCel6A) [13] and chitinase A from bacterium *Serratia marcescens* (SmChiA) [14]. In both methods, the stepping motions of the enzymes were not resolved due to the low temporal resolution and localization precision. Revealing the moving mechanisms of processive chitinases and cellulases is helpful for making mutants with a higher activity than wild type or improving the reaction conditions for utilization of biomass.

Recently, we succeeded in observing the stepping motion of SmChiA labeled by a gold nanoparticle (Fig. 1) [15]. Our results revealed that SmChiA is a burnt-bridge Brownian ratchet motor, which hydrolyzes a molecular chain of chitin to disaccharides. In this review, we will introduce the recent progress obtained by high-speed and high-precision single-molecule measurement.

Precision and temporal resolution of TIRDF-microscopy with gold nanoparticles

In the biochemical assay, the main product of chitin hydrolysis by SmChiA is N,N'-diacetyl chitobiose (written as chitobiose in the following), which is the repeating unit of the chitin molecular chain [16]. This indicates that SmChiA hydrolyzes the chitin chain to each chitobiose unit with a processive motion. The theoretical length of chitobiose is about 1 nm. Thus, the expected step size of

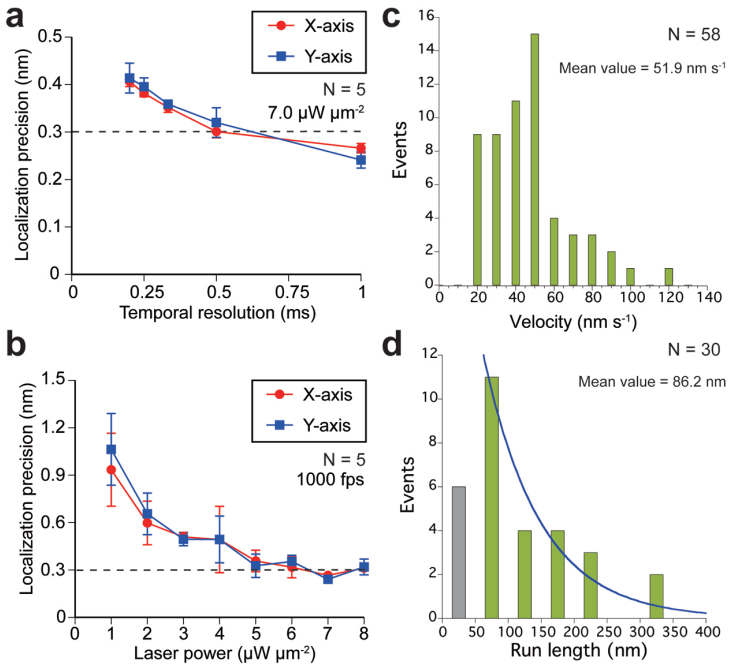

Figure 2 Evaluation of the observation system. (a) Relationship between localization precision and temporal resolution at 7 μW μm^{-2} with a 40-nm gold nanoparticle. (b) Relationship between localization precision and laser power at 1000 fps with a 40-nm gold nanoparticle. (c) Moving velocity of SmChiA labeled by a 40-nm gold nanoparticle. (d) Moving length of SmChiA labeled by a 40-nm gold nanoparticle.

SmChiA is also 1 nm. This step size is smaller than those of kinesin 1, dynein along the on-axis (~8 nm) or skeletal myosin (4–5 nm) [17]. This smaller step size is one reason for the difficulty in observing the stepping motion of SmChiA by single-molecule fluorescence imaging or HS-AFM. The other factor is the expected dwell time of steps. Given the moving velocities of SmChiA observed by HS-AFM (70 nm s^{-1}) and single fluorescence imaging (52 nm s^{-1}), the expected dwell time of each step is roughly 14 to 19 ms. Previous observation rates in HS-AFM and single-molecule fluorescence imaging were 7 and 3 frames per second (fps), respectively. These observation rates corresponded to the 142 and 333 ms in temporal resolutions, which were not enough to resolve single reactions of SmChiA. Using total internal reflection dark-field (TIRDF) microscopy [18], we achieved 0.3-nm localization precisions in both X- and Y-axes at 2000 fps (0.5-ms temporal resolution) with 7.0 μW μm^{-2} laser power density (Fig. 2a). To check the limit of localization precision of our system, gold nanoparticles with a diameter of 40 nm were stabilized on a coverslip by sodium chloride solution and illuminated by the evanescent field of a 532-nm laser with various power densities under 1000 fps recording (Fig. 2b). When the power density of incident laser was increased, precisions in the X- and Y-axes were improved, but they saturated at around 0.3 nm for above 5.0 μW μm^{-2}.

The localization precision (σ) can be theoretically calculated as a function of experimentally measurable values [19].

$$\sigma = \sqrt{\frac{s^2 + a^2/_{12}}{N} + \frac{8\pi s^4 b^2}{a^2 N^2}}$$

where s is the standard deviation of the point-spread function (width of the particle image), N is the detected photon number, a is the finite pixel size of the detector, and b is the standard deviation of background intensity. The first term is the error of measurement of photons including the limitation of finite pixel size of the camera. The second term is the effect of background noise. Practically, the first term in the equation becomes dominant under high laser power conditions [20]. The localization precision should be improved when N was increased, but the precision saturated at around 0.3 nm in actual measurements. This limitation of precision was caused by the charge-saturation of the pixels of the camera. After saturation, the photons were not detected, and the value of N did not increase. Recently, use of a two-times higher magnification and a smaller pixel size, with photons in one pixel being shared in four pixels, enabled us to improve the precision up to 0.13 nm at 30 μW μm^{-2} input from an annular-shaped laser and 1-ms temporal resolution [20]. Higher precision is better for observation, but too much laser power denatures the target protein. For the measurement of SmChiA, we used 7.0 μW μm^{-2} and 0.3-nm precision at 0.5-ms temporal resolution with 67.6 nm per pixel. Under these conditions, the localization precision was about 0.3 nm and was enough to resolve the 1-nm stepping. In addition, the moving velocity and moving length of SmChiA with a gold nanoparticle

were 51.9 nm s^{-1} and 86.2 nm, respectively (Fig. 2c and d). These values were similar to or longer than those of a fluorescence-labeled enzyme (52.7 nm s^{-1} and 60.4 nm) previously reported [14]. These results indicated that our observation conditions did not damage the SmChiA molecules. Moreover, the similarity of the moving velocities between the gold nanoparticle and fluorescence-dye-labeled SmChiA also proved that the 40-nm gold nanoparticle did not inhibit the movement of SmChiA. From the Stokes–Einstein relation, the diffusion coefficient of a spherical particle is written as

$$D = \frac{k_B T}{6\pi\eta a}$$

where k_B is the Boltzmann constant (1.38×10^{-23} J K^{-1}), T is temperature, η is the viscosity of the solvent, and a is the radius of the sphere. The viscosity of water at 25°C is 0.890 mPa s; hence, D of a gold nanoparticle of 40-nm diameter is 1.23×10^{-11} m^2 s^{-1}. During one second, the particle moves on average ~5 μm along an axis. This value is almost a hundred times larger than the moving length of SmChiA in a second; thus, a gold nanoparticle of 40 nm diameter does not inhibit the movement of SmChiA.

Observation and analysis of the stepping motion of SmChiA

Biotinylated SmChiA G157C-V351C and streptavidin-coated gold nanoparticles (and PEG) were mixed in the same molar ratio and connected to each other by 1-hour incubation at 25°C in a tube. Crystalline beta-chitin fibrils purified from tubes of *Lamellibrachia satsuma* were stabilized on a coverslip by a spin coater. The coverslips were washed and rinsed with 10 M potassium hydroxide and milliQ water before use. A flow cell was constructed with the chitin-coated glass and a smaller coverslip. Fibrils were observed by the scattering images of a 532-nm laser at 500 fps, and a suitable position (high density of fibrils, but low overlaps and aggregations) for measurement of SmChiA movement was determined. The suspension of gold nanoparticles with SmChiA was loaded into the cell, and a movie was taken at 2000 fps after stopping the cooling fan of the camera. The recorded movie was checked manually. The image area including the moving molecules on the chitin fibril was used for further analysis. A stationary particle in the same field of view was used as a reference of stage drift, and the data containing the effect of stage drift was excluded from the analysis. A trace of the particle was analyzed by 2D Gaussian fitting of images. The obtained trace was transformed by the below functions to separate the moving axis (on-axis) and non-moving axis (off-axis).

$$Xon = \cos\theta \times Xraw + \sin\theta \times Yraw$$

$$Yoff = -\sin\theta \times Xraw + \cos\theta \times Yraw$$

where θ is the angle between the X_{on} and X_{raw} axes. The velocity was analyzed as the slope of the linear fit from the starting and stopping points. The moving length was calculated as the distance between the two points. The traces were smoothed by the moving median of displacements during ±2 ms. The median treated trace was analyzed by the step finding algorithm, and the step trace that showed a peak of fitting score was chosen [21]. Any trace did not show a peak was not used. In the stepping trace, the periods of pauses were known. Therefore, we estimated the precision of gold attached to SmChiA from the deviation of positions during the pauses. The precisions of the particle along the on-axis with and without median smoothing were 0.34±0.18 nm and 0.67±0.21 nm, respectively. Median smoothing removed the effect of fluctuations of SmChiA and the linker region, because the precision after median smoothing was similar to that of a gold nano-particle attached on the glass surface.

An example trace of the stepping molecule is shown in Figure 3a. The molecule showed a linear motion along the on-axis and a small movement along the off-axis. The detected stepping trace fitted well with the raw and median smoothed traces. Basically, the molecule showed continuous forward steps, but sometimes a backward step and recovery steps from the backward state were also observed (Fig. 3b and c). These steps were analyzed separately, because the states of enzyme and chitin chain might have been different. The elementary steps of SmChiA expected during the processive movement are (1) hydrolysis of chain, (2) release of product, and (3) waiting for decrystallization of the chitobiose unit and reformation of the Michaelis complex. Considering these cycles of reaction, the backward step and recovery step correspond to the dissolution and reformation of the Michaelis complex with recrystallization and decrystallization of the chitobiose unit, respectively. At first, the distribution of step sizes (distance between two pauses) of the forward and backward steps was analyzed (Fig. 3d). The main peaks of the forward and backward steps were 1.1 and –1.1 nm, respectively. These distributions highly indicated that SmChiA recognizes the chitobiose units during the movement. Additionally, the steps also showed a peak at 2.2 nm. The steps larger than 2 nm could be the steps skipping a chitobiose unit or just a failure to observe the 1-nm step. This event was evaluated after analysis of time constants. The higher ratio of forward (83.5%) than backward steps (16.5%) indicated the moving direction of SmChiA is biased forward. Next, the distributions of dwell times (waiting time before the stepping motion) of each step were analyzed. That of the forward steps showed a peak and was fitted by the difference of two exponential decay functions corresponding to the sequential reaction (Fig. 4a). The obtained time constants were 23.9±2.1 ms and 2.9±1.0 ms, respectively. To determine the elementary step with a shorter time constant, SmChiA was also observed in D_2O. The hydrolysis reaction needs the

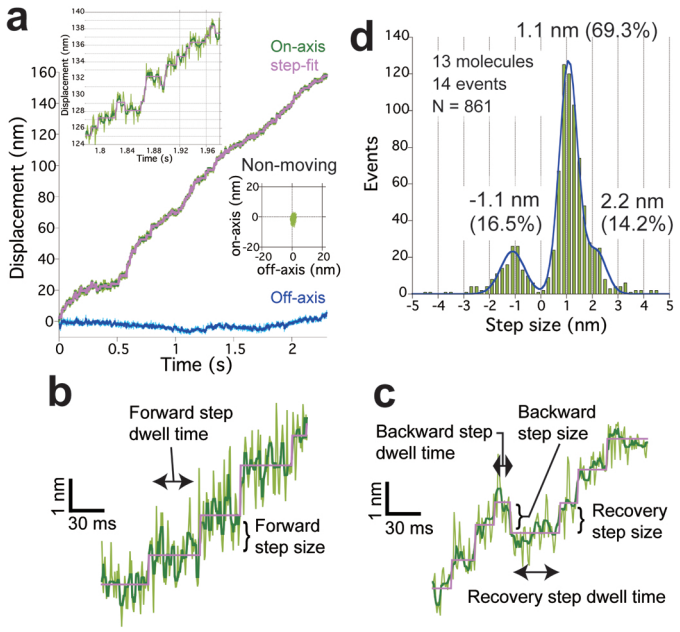

Figure 3 Observation of SmChiA labeled by a gold nanoparticle. (a) Example of the stepping movement of SmChiA. (b) Example of continuous forward steps. (c) Example of backward and recovery steps. (d) Distribution of step size for forward and backward steps.

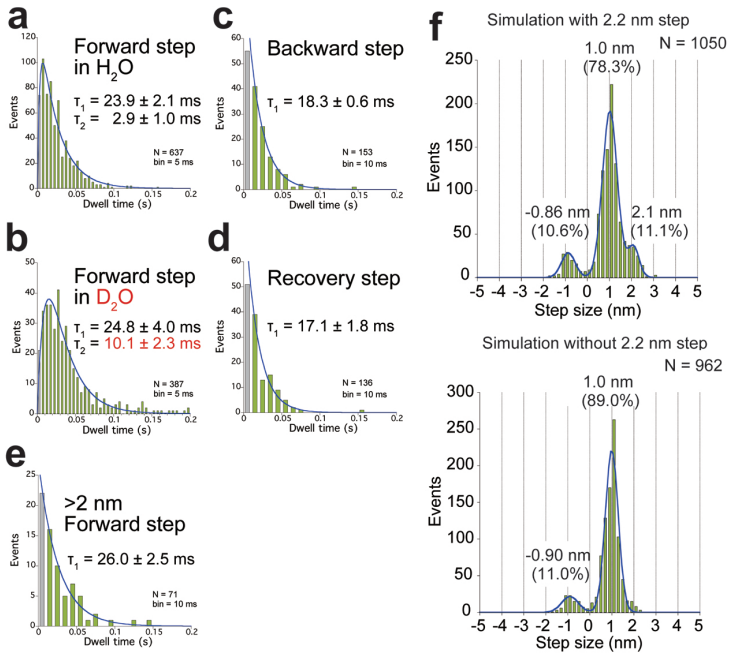

Figure 4 Time constants analysis and evaluation of 2-nm steps. (a–e) Distributions of dwell times. (f) Distributions of step size detected in the simulation with or without 2-nm steps.

D_2O molecule as a substrate to exchange the D–O bond between D_2O and chitin. Therefore, the time constant including hydrolysis was extended to 10.1±2.3 ms from 2.9 ms due to the kinetic isotope effect (Fig. 4b). The other long time constant (23.9 ms) might be the sum of the time constants of product release and formation of the Michaelis complex by decrystallization. Distributions of dwell times of backward and recovery steps were fitted by single exponential decay functions. Their time constants were 18.3±0.6 ms and 17.1±1.8 ms, respectively (Fig. 4c and d). Similar values of these time constants indicated that the backward and forward states are at a similar level on the free energy

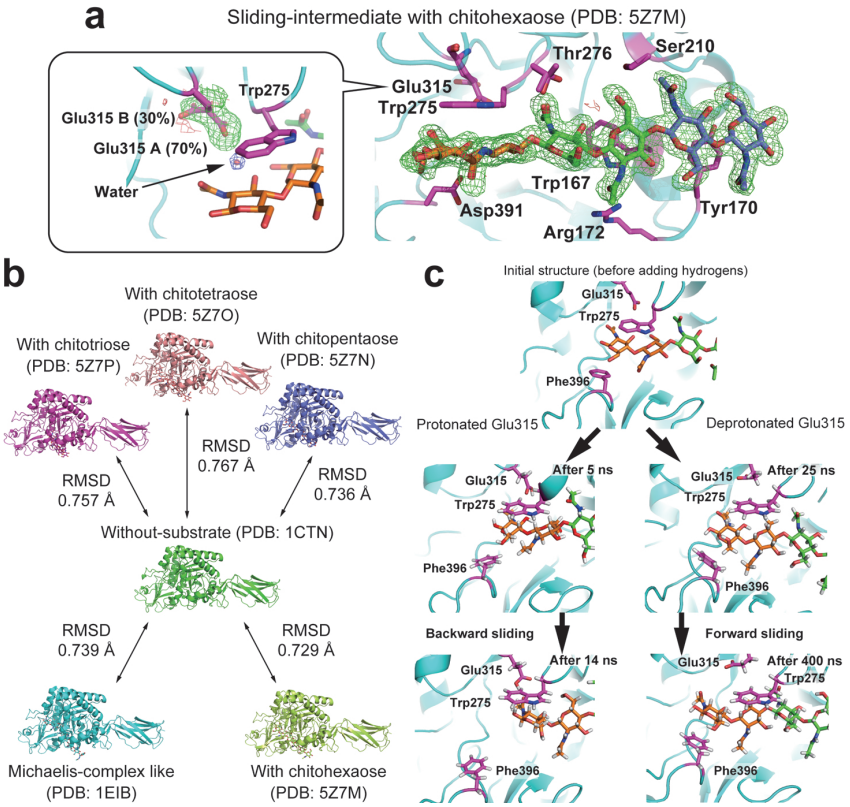

Figure 5 Structural analysis of SmChiA. (a) Sliding intermediate structure of SmChiA with chitohexaose. (b) Comparison of structures of SmChiA intermediate states and the substrate-free structure. (c) Molecular dynamics simulations of SmChiA.

profile. Thus, SmChiA can move back and forth by thermal diffusion along the chain. Moreover, the elemental reaction of the recovery step is the same as the formation of the Michaelis complex by decrystallization in the forward step. Therefore, the time constant of product release was estimated as the difference of time constants of the recovery step and the longer time constant of the forward steps (23.9–17.1=6.8 ms). Among the elementary steps, the hydrolysis and the dissolution of the Michaelis complex are in competition with the forward stepped state. The reaction ratio was determined by the ratio of time constants, and that of hydrolysis was estimated as 86.3%. This ratio is very close to the ratio of the forward steps determined by the events ratio (83.5%=69.3%+14.2%). This result indicated that SmChiA is biased forward due to the faster hydrolysis of the chain than the release of the chain from the active site. After the hydrolysis, the chitobiose unit is released, and the chain is shortened by 1 nm. This change causes the inhibition of the backward step, because SmChiA cannot make a stable backward state anymore. This system for creating a bias of movement is called a “burnt-bridge” mechanism [22].

The dwell time of forward steps larger than 2 nm was 26.0±2.5 ms and similar to that of the 1-nm forward step (Fig. 4e). This result indicated that decrystallization of one chitobiose unit occurred during a 2-nm step. Chitin is a repeat of N,N'-diacetyl chitobiose, but acetylation of the amides is not complete, especially on the surface of the crystal. Without the acetyl group, the chitobiose unit cannot make a hydrogen bond with neighboring chains. Additionally, SmChiA uses the acetyl group of chitin as a catalytic nucleophile, and the oxygen atom of the acetyl group attacks the C1 carbon to cleave the glycoside bond and make the cyclic intermediate structure. This reaction mechanism, using part of the substrate as a catalyst, is called substrate assisted catalysis [23]. One possibility for the 2-nm step is to skip past one non-crystallized and deacetylated chitobiose unit without hydrolysis of the chain. The other possibility, failure to observe the very fast 1-nm step, was not so significant, because 2-nm steps were detected only in the trajectories generated by kinetic simulations including the events of the 2-nm step (Fig. 4f).

Sliding intermediate structure and molecular dynamics simulation

To investigate the moving mechanism of SmChiA, we also tried to solve the X-ray crystal structure of the sliding-intermediate state of SmChiA. A Michaelis-complex like structure was used as a reference, and we additionally

mutated the residues stabilizing the complex to get a less stable complex structure. Crystals of the mutant were soaked in the crystallization reagents from chitotriose to chitohexaose, and the diffraction spots were collected under cryo-conditions. The complex with hexaose showed stacking of the reducing end of the chain on Trp275 (Fig. 5a). The chain was twisted between the second and third rings from the reducing end, and the chitobiose unit existed on the same plane as the product binding site. Therefore, this structure resembled one of the stable states of the sliding intermediate. Although the complexes with shorter oligosaccharides kept the chains in various positions and resembled a part of sliding intermediates, the structures of SmChiA were similar to those without the substrate (Fig. 5b). This result indicated that SmChiA moves without large structural changes of the enzyme.

The sliding-intermediate structure with hexaose was used as a template, and molecular dynamics simulations were performed to observe the sliding motion of the chain. In the simulation, protonated and deprotonated Glu315 residues were prepared, because the catalytic acid/base residue Glu315 showed double conformers in the structure (Fig. 5a). In the deprotonated initial structure, Glu315 oriented to the inside of the cleft, and the chain moved to the forward direction (Fig. 5c). The reducing end of the chain was stacked on Phe396, which is the residue of the product binding site. In contrast, in the protonated structure, protonated Glu315 interacted with the reducing end of the chain and stabilized the backward state. Both movements were caused by thermal fluctuations. From these results, SmChiA was revealed as a "burnt-bridge" Brownian ratchet motor.

In the single-molecule measurement, the backward and forward stepped states were estimated as having a similar free energy level. The molecular dynamics simulations gave us the backward state complex. And, the forward stepped state had been reported as the Michaelis complex. The large difference between the two structures is the interaction at product sites (subsite +1 and +2). This difference favors stabilization of the forward stepped state than the backward state. Although these results focused only on the interaction between enzyme and the single chain, they were the results of a single-molecule analysis including the change of crystalline chitin: decrystallization and recrystallization. The energy of decrystallization of the chitobiose unit was previously estimated as 6–8 kcal mol^{-1} [24]. Consequently, SmChiA provides this energy by the binding energy at the product sites and stabilizes the decrystalized state of the chain.

Comparison of moving mechanisms among SmChiA and other linear motors

Two well-studied linear motor proteins are conventional kinesin and myosin, which have a mixture of power stroke and Brownian-ratchet mechanisms. In the former case, a neck linker interacts with the C-terminus of the head domain and forms a partial β-strand after binding of ATP [25]. This structural change causes the directional diffusion of the other head and rectifies the moving direction of the motor molecule. A Brownian-ratchet mechanism changes the conformation of the lever arm in conjunction with ATP hydrolysis by the head and dissociation of products to generate the bias of moving direction [26]. These two motors have different force generation steps, but the heads of both motors repeat the binding and dissociation steps from the rail proteins (tubulin and actin filaments, respectively), and molecules move along those rails. In contrast, SmChiA keeps the binding state and degrades the rail during the movement. Instead of a conformational change of the protein, the structure of the rail sugar chain is changed to make the bias of moving direction. Given that these linear motors move with a rectified Brownian motion, the difference among them seems to be only in the way to create the bias for the diffusion.

Conclusion

The 1-nm steps of SmChiA were resolved, and the time constants of the elementally steps were determined by high-precision and time-resolution imaging using gold nanoparticles. Additionally, the combination of single-molecule measurement by X-ray crystallography and molecular dynamics simulations revealed that SmChiA is a "burnt-bridge" Brownian ratchet motor. This mechanism is well designed for the degradation of polymer substrates. Additionally, this "burnt-bridge" Brownian ratchet may be a common mechanism, because of the abundance of polymers in the world such as cellulose, collagen, hyaluronic acid, and DNA. We hope to construct an artificial molecular motor and verify the moving mechanism using high-precision single molecule observation with plasmonic nano probes.

Acknowledgments

We thank Y. Niitani (Nikon) and M. Tomishige (Aoyama Gakuin Univ.) for the step-finding algorithm plugin for ImageJ, and H. Ueno (Univ. Tokyo) for discussion about gold nanoparticle coating. X-ray diffractions were measured at BL2S1 in AichiSR.

Conflicts of Interest

All authors declare that they have no conflict of interest.

Author Contributions

A.N. wrote the manuscript. K. O., T. F., M. S., J. A. and R. I. reviewed the manuscript and approved the final form.

References

[1] Lipowsky, R. & Klumpp, S. 'Life is motion': multiscale motility of molecular motors. *Physica A* **352**, 53–112 (2005). DOI: 10.1016/j.physa.2004.12.034

[2] Isojima, H., Iino, R., Niitani, Y., Noji, H. & Tomishige, M. Direct observation of intermediate states during the stepping motion of kinesin-1. *Nat. Chem. Biol.* **12**, 290–297 (2016). DOI: 10.1038/nchembio.2028

[3] Ando, J., Shima, T., Kanazawa, R., Shimo-Kon, R., Nakamura, A., Yamamoto, M., *et al.* Small stepping motion of processive dynein revealed by load-free high-speed single-particle tracking. *Sci. Rep.* **10**, 1080 (2020). DOI: 10.1038/s41598-020-58070-y

[4] Kodera, N., Yamamoto, D., Ishikawa, R. & Ando, T. Video imaging of walking myosin V by high-speed atomic force microscopy. *Nature* **468**, 72–76 (2010). DOI: 10.1038/nature09450

[5] Fujita, K., Ohmachi, M., Ikezaki, K., Yanagida, T. & Iwaki, M. Direct visualization of human myosin II force generation using DNA origami-based thick filaments. *Commun. Biol.* **2**, 437 (2019). DOI: 10.1038/s42003-019-0683-0

[6] Okuno, D., Iino, R. & Noji, H. Rotation and structure of FoF1-ATP synthase. *J. Biochem.* **149**, 655–664 (2011). DOI: 10.1093/jb/mvr049

[7] Ueno, H., Minagawa, Y., Hara, M., Rahman, S., Yamato, I., Muneyuki, E., *et al.* Torque generation of Enterococcus hirae V-ATPase. *J. Biol. Chem.* **289**, 31212–31223 (2014). DOI: 10.1074/jbc.M114.598177

[8] Nakanishi, A., Kishikawa, J., Tamakoshi, M. & Yokoyama, K. The ingenious structure of central rotor apparatus in VoV1; key for both complex disassembly and energy coupling between V1 and Vo. *PLoS One* **10**, e0119602 (2015). DOI: 10.1371/journal.pone.0119602

[9] Hwang, W. & Karplus, M. Structural basis for power stroke vs. Brownian ratchet mechanisms of motor proteins. *Proc. Natl. Acad. Sci. USA* **116**, 19777–19785 (2019). DOI: 10.1073/pnas.1818589116

[10] Garcia, M. A. Surface plasmons in metallic nanoparticles: fundamentals and applications. *J. Phys. D Appl. Phys.* **44**, 283001 (2011). DOI: 10.1088/0022-3727/44/28/283001

[11] Igarashi, K., Uchihashi, T., Koivula, A., Wada, M., Kimura, S., Okamoto, T., *et al.* Traffic jams reduce hydrolytic efficiency of cellulase on cellulose surface. *Science* **333**, 1279–1282 (2011). DOI: 10.1126/science.1208386

[12] Igarashi, K., Uchihashi, T., Uchiyama, T., Sugimoto, H., Wada, M., Suzuki, K., *et al.* Two-way traffic of glycoside hydrolase family 18 processive chitinases on crystalline chitin. *Nat. Commun.* **5**, 3975 (2014). DOI: 10.1038/ncomms4975

[13] Nakamura, A., Tasaki, T., Ishiwata, D., Yamamoto, M., Okuni, Y., Visootsat, A., *et al.* Single-molecule Imaging Analysis of Binding, Processive Movement, and Dissociation of Cellobiohydrolase Trichoderma reesei Cel6A and Its Domains on Crystalline Cellulose. *J. Biol. Chem.* **291**, 22404–22413 (2016). DOI: 10.1074/jbc.M116.752048

[14] Nakamrua, A., Tasaki, T., Okuni, Y., Song, C., Murata, K., Kozai, T., *et al.* Rate constants, processivity, and productive binding ratio of chitinase A revealed by single-molecule analysis. *Phys. Chem. Chem. Phys.* **20**, 3010–3018 (2018). DOI: 10.1039/C7CP04606E

[15] Nakamura, A., Okazaki, K. I., Furuta, T., Sakurai, M. & Iino, R. Processive chitinase is Brownian monorail operated by fast catalysis after peeling rail from crystalline chitin. *Nat. Commun.* **9**, 3814 (2018). DOI: 10.1038/s41467-018-06362-3

[16] Zakariassen, H., Aam, B. B., Horn, S. J., Vårum, K. M., Sørlie, M. & Eijsink, V. G. H. Aromatic Residues in the Catalytic Center of Chitinase A fromSerratia marcescensAffect Processivity, Enzyme Activity, and Biomass Converting Efficiency. *J. Biol. Chem.* **284**, 10610–10617 (2009). DOI: 10.1074/jbc.M900092200

[17] Kaya, M., Tani, Y., Washio, T., Hisada, T. & Higuchi, H. Coordinated force generation of skeletal myosins in myofilaments through motor coupling. *Nat. Commun.* **8**, 16036 (2017). DOI: 10.1038/ncomms16036

[18] Ueno, H., Nishikawa, S., Iino, R., Tabata, K. V., Sakakihara, S., Yanagida, T., *et al.* Simple dark-field microscopy with nanometer spatial precision and microsecond temporal resolution. *Biophys. J.* **98**, 2014–2023 (2010). DOI: 10.1016/j.bpj.2010.01.011

[19] Thompson, R. E., Larson, D. R. & Webb, W. W. Precise Nanometer Localization Analysis for Individual Fluorescent Probes. *Biophys. J.* **82**, 2775–2783 (2002). DOI: 10.1016/S0006-3495(02)75618-X

[20] Ando, J., Nakamura, A., Visootsat, A., Yamamoto, M., Song, C., Murata, K., *et al.* Single-Nanoparticle Tracking with Angstrom Localization Precision and Microsecond Time Resolution. *Biophys. J.* **115**, 2413–2427 (2018). DOI: 10.1016/j.bpj.2018.11.016

[21] Kerssemakers, J. W. J., Munteanu, E. L., Laan, L., Noetzel, T. L., Janson, M. E. & Dogterom, M. Assembly dynamics of microtubules at molecular resolution. *Nature* **442**, 709–712 (2006). DOI: 10.1038/nature04928

[22] Mai, J., Sokolov, I. M. & Blumen, A. Directed particle diffusion under "burnt bridges" conditions. *Phys. Rev. E Stat. Nonlin. Soft Matter Phys.* **64**, 011102 (2001). DOI: 10.1103/PhysRevE.64.011102

[23] Terwisscha van Scheltinga, A. C., Armand, S., Kalk, K. H., Isogai, A., Henrissat, B. & Dijkstra, B. W. Stereochemistry of chitin hydrolysis by a plant chitinase/lysozyme and X-ray structure of a complex with allosamidin: evidence for substrate assisted catalysis. *Biochemistry* **34**, 15619–15623 (1995). DOI: 10.1021/bi00048a003

[24] Beckham, G. T. & Crowley, M. F. Examination of the α-Chitin Structure and Decrystallization Thermodynamics at the Nanoscale. *J. Phys. Chem. B* **115**, 4516–4522 (2011). DOI: 10.1021/jp200912q

[25] Hwang, W., Lang, M. J. & Karplus, M. Force generation in kinesin hinges on cover-neck bundle formation. *Structure* **16**, 62–71 (2008). DOI: 10.1016/j.str.2007.11.008

[26] Trybus, K. M. Myosin V from head to tail. *Cell Mol. Life Sci.* **65**, 1378–1389 (2008). DOI: 10.1007/s00018-008-7507-6

(*Edited by Tamiki Komatsuzaki*)